2D open loop trajectory control of a micro-object in a dielectrophoresis-based device.

Mohamed Kharboutly, Alexandre Melis, Michaël Gauthier, Nicolas Chaillet

2D open loop trajectory control of a micro-object in a dielectrophoresis-based device

Mohamed Kharboutly[1] Alexandre Melis[1] , Michaël Gauthier[1] , *Member, IEEE,*
Nicolas Chaillet[1] , *Member, IEEE,*

***Abstract*— In the last years, industries have shown a global trend to miniaturize the size of the components to micron in order to reduce the dimension of the final product. At this scale, a micro-object behaves differently from the micro-scale and its behavior is affected by additional physical phenomenon such as the dielectrophoresis. Dielectrophoresis (DEP) is used to separate, manipulate and detect micro particles in several domains with high speed and precision, such as in biological cell or Carbon Nano-Tubes (CNTs) manipulations. This paper focuses on developing a $2D$ direct dynamic model of the micro-object behavior on the base of a $3D$ dielectrophoretic simulator. This $2D$ dynamic model is used to establish an open loop control law by a numerical inversion. Exploiting this control law, a high speed trajectory tracking and high precision positioning can be achieved. Several simulated and experimental results are shown to evaluate this control strategy and discuss its performance.**

I. Introduction

High speed transportation and high precision assembly of industrial components can be achieved using conventional ways such as vacuum gripper and motorized conveyor. In the last years, industries have shown a global trend to miniaturize the size of the components to micron in order to reduce the dimension of the final product. At this scale, a micro-object behaves differently from the micro-scale and its behavior is affected by additional physical phenomenon [1]. Some of these phenomenons can be exploited and used to transport micro-objects without any direct contact [2], [3], [4]. In fact, at this scale, the forces created by these phenomenons can be greater than the micro-object's weight and micro-objects move in levitation ensuring no contact with any surface.

One of the phenomenon used at this scale is the dielectrophoresis where micro particles can be transported, in a liquid medium, without contact from location to another with high-speed motion and precision [5]. Dielectrophoretic force is a force which requires a non-uniform electric field and is proportional to its gradient's square. In general, by applying an electric voltage on electrodes characterized by its geometry can creates this electric field [6]. Dielectrophoresis is used either in a liquid flow [7] or stable liquid medium [8], and can be either negative or positive depending on the electric permittivity and conductivity of the particle and the liquid medium and the electric field frequency. Positive dielectrophoresis generates a force directed from the particle to the electrode (attractive force), and negative dielectrophoresis applies a force directed from electrodes toward the particle (repulsive force). This characteristic makes possible to separate different kind of particles such as biological cell mixed in one liquid flow by choosing the appropriate frequency which applies positive dielectrophoresis on some cells, and negative dielectrophoresis on others [9]. It can also be used to capture particles by applying positive dielectrophoresis [10] and attract and position carbon nano-tubes (CNTs) [11], [12]. Another use of this force consists in transporting and precisely positioning and orienting of micro-objects using negative dielectrophoresis [13], [14], [15].

Current micro-manipulation on dielectrophoresis-based devices captures particles by creating only one stable point in the space. These devices do not offer the ability to control the object's trajectory neither its final equilibrium stable position. Moreover, the motion range is limited to a very small distance compared to the micro-object dimension.

Using periodic structure of electrodes presented in the figure 1, micro-objects can be transported separately along long distances with high speed and precision using negative dielectrophoresis. For this aim, an appropriate control strategy is needed. This control strategy might be divided into two levels. A local control law, controlling the micro-bead's trajectory in a local periodic electrode structure, and a global control law controlling the trajectory of the micro-bead from structure to another. This paper focuses on developing a numerical model of the micro-bead's behavior and the local control law based on the numerical model. Simulation and experiments are also presented in the last section.

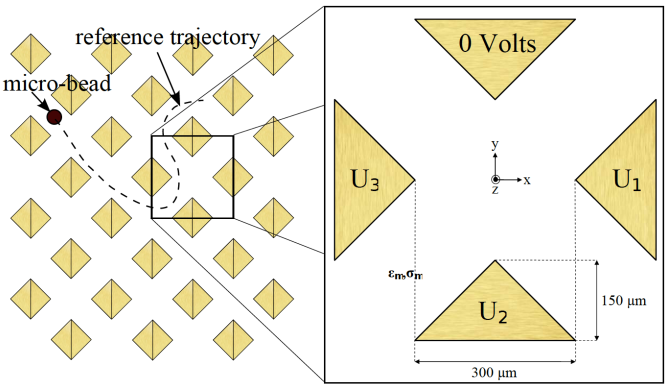

Fig. 1. Geometric shape of electrodes

[1] FEMTO-ST Institute, AS2M dept. UMR CNRS 6174 - UFC/ENSMM/UTBM, 24 rue Alain Savary, 25000, Besançon, France

II. Direct dynamic Model of a dielectrophoresis-based system

In this section, we present a $3D$ dielectrophoretic force simulator applied on a micro-bead, which will be used as reference system. Secondly, a 2D direct dynamic model based on the $3D$ dielectrophoretic force simulator, will be presented and used to establish a 2D control law presented in the next section.

A. Dielectrophoresis force similator

In order to compute the electric field and then the dielectrophoretic force applied to a micro-object in an electrode structure, a numerical simulator is needed. This numerical simulator must be able to compute the dielectrophoretic force generated by very complex geometries in a very short time. For one hand, corresponding analytic equations are very complex and hard to be established. For a second hand, the finite element modeling (FEM) solution is limited to a long computation time and specially when electric voltage changes frequently. Thus, we propose to use the hybrid numeric simulator proposed in [16] gathering the ability of the FEM solution to simulate complex electrodes geometry and the short computation time of the analytical equations. According to [6], the dielectrophoretic force $\overrightarrow{F}_{DEP}$ applied to the micro-bead's center $X(x,y,z)$ with respect to the electric field $\overrightarrow{E}(X,U)$ can be written as:

$$\overrightarrow{F}_{DEP}(X,U) = 2\pi\epsilon_m r^3 Re[K(\omega)]\nabla(\overrightarrow{E}^2(X,U)), \quad (1)$$

where

$$K(\omega) = \frac{\epsilon_p^* - \epsilon_m^*}{\epsilon_p^* + 2\epsilon_m^*}, \quad (2)$$

and ϵ_p^* and ϵ_m^* are respectively the complex permittivity of the particle and the medium with:

$$\epsilon^* = \epsilon + j\frac{\sigma}{\omega}, \quad (3)$$

ϵ is the relative permittivity, σ is the conductivity and ω is the angular velocity of the electric field. Thus, if we consider a configuration of n electrodes, by applying $n-1$ sinusoidal electric voltages identified by there magnitudes $U = [U_1, ...U_{n-1}]$ and there angular velocity ω, the electric field $\overrightarrow{E}(X,U)$ can be computed using the hybrid method described in [16]. This hybrid method consists in computing the electric field $\overrightarrow{E}(X,U)$ by integrating the surface charge density on the electrodes. In fact the electric charge density Q and the magnitudes of the applied voltages U on the electrodes are linearly related:

$$Q = \sum_{i=1}^{n-1}(C_i U_i), \quad (4)$$

where U_i is the magnitude of the applied voltage on the ith electrode and C_i is the elementary inter-capacitance between the electrodes influenced by the ith electrode. The inter-capacitance between the electrodes depends on only the geometric shape of the electrodes and the electric permittivity of the medium. The C_i is simulated using FEM software. These simulations are executed in preprocessing which reduces the total time of the force computation. If we consider the electrodes presented in the figure 1, the number of electrodes n is equal to 4 and they are placed in the x,y plane.

To compute the electric charge density Q with respect to the applied voltages $U = [U_1, U_2, U_3]$, $n-1 = 3$ FEM simulations are required. The figures 2(a) and 2(b) show the elementary inter-capacitances C_1 and C_3. The figure 2(c) shows how the electric charge density Q is analytically computed with respect to the applied voltages $U = [75V, 0, 75V]$ and the elementary inter-capacitances C_1 and C_3.

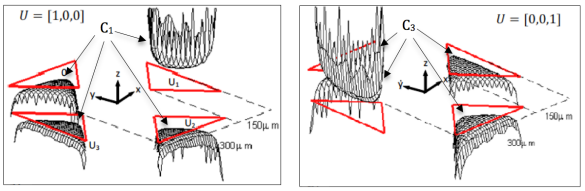

(a) Elementary inter-capacitance C_1. (b) Elementary inter-capacitance C_3.

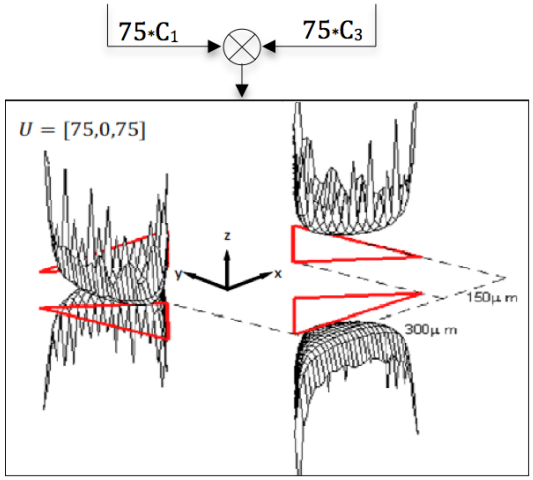

(c) The computed charge density $C = 75 \times C_1 + 75 \times C_3$.

Fig. 2. The electric charge density computed on the electrodes by applying the following electric voltages: $U = [75V, 0, 75V]$.

Once the matrix of the electric charge density Q is computed, the electric field can be calculated analytically in a point $X(x,y,z)$ in the medium. In fact, with each value $Q_{i,j}$ of the computed matrix Q corresponds a $x_{i,j}$, $y_{i,j}$ point on the electrodes ($z_{i,j} = 0$ because of the electrodes are in the x,y plane). Thus, the expression of the electric field $\overrightarrow{E}$ at the point $X(x,y,z)$ is:

$$\overrightarrow{E}(x,y,z) = \sum_i \left(\sum_j \frac{Q_{i,j}\overrightarrow{r}}{4\pi\epsilon_m \| \overrightarrow{r} \|^3} \right), \quad (5)$$

where $r = [x - x_{i,j}, y - y_{i,j}, z]$, and the DEP force can be also computed analytically with respect to (1). The figure 3 resumes the DEP modeling simulator (DMS) block. The block's inputs are the geometric shape of the electrodes, the

applied voltages and the micro-bead's current position. This block generates the computed x, y and z components of the dielectrophoretic force applied to the micro-bead in its center.

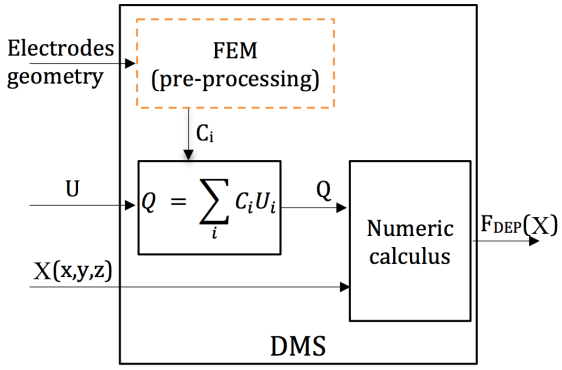

Fig. 3. DEP modeling simulator (DMS).

B. $3D$ direct dynamic model

The dynamic of a micro-bead in motion under dielectrophoretic force field, in a liquid medium is ruled by the following dynamic equation:

$$\overrightarrow{F}_{DEP}(X) + \overrightarrow{F}_{Drag} + \overrightarrow{P} = m\ddot{\overrightarrow{X}}, \tag{6}$$

where X is the space coordinates of the micro-bead's center $X(x, y, z)$, $\dot{X}$ is its velocity, $\ddot{X}$ its acceleration, $\overrightarrow{F}_{DEP}(X)$ is the applied dielectrophoretic force on the center of the micro-bead, $\overrightarrow{P}$ is its apparent weight, m is its mass and $\overrightarrow{F}_{Drag}$ is the viscosity friction created on the micro-bead. Generally, in the micro-scale, micro-manipulation in a liquid medium with dynamic viscosity ν is characterized by a Reynolds number much smaller than 1. In this case the micro-bead's inertia impact is very small compared to the viscosity friction $\overrightarrow{F}_{Drag}$. Thus the inertia term $m\ddot{\overrightarrow{X}}$ can be neglected and the dynamic equation becomes:

$$\overrightarrow{F}_{DEP}(X) + \overrightarrow{F}_{Drag}(\dot{X}) + \overrightarrow{P} = 0. \tag{7}$$

In the micron scale the Stokes approach of the viscosity friction is valid, $\overrightarrow{F}_{Drag}(\dot{X})$ becomes:

$$\overrightarrow{F}_{Drag}(\dot{X}) = -6\pi\nu R\dot{\overrightarrow{X}} \tag{8}$$

and the dynamic equation is thus:

$$\dot{\overrightarrow{X}} = \frac{\overrightarrow{F}_{DEP}(X) + \overrightarrow{P}}{6\pi\nu R}. \tag{9}$$

The diagram in the figure 4 illustrates the $3D$ direct dynamic modeling. Having the applied electric voltages and the electrodes geometry as input, the direct modeling simulator computes the corresponding micro-bead's trajectory. In generally, the micro-bead's behavior in dielectrophoretic force field is characterized by its high dynamics and nonlinearity. This numeric simulator is experimentally validated in [16] where we have shown that the dynamics are very high and the time response of the micro-bead is less than $3ms$. Moreover the behavior of the micro-bead is subjected to a high nonlinearity and especially when the micro-bead approaches the electrodes.

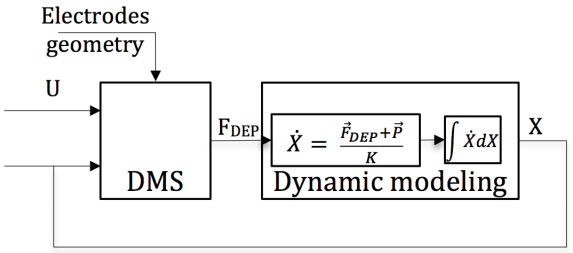

Fig. 4. A dynamic modeling and DMS are used to compute the micro-bead's 3D trajectory.

C. $2D$ simplified dynamic model

In order to reduce the complexity of the computation, we will consider that the electrodes surface is planar in the x, y plane. The $3D$ dielectrophoretic dynamic modeling simulator is designed to run on a classic PC with high performance (typically GHz) and it is not optimized to be integrated directly into a controller card with lower calculation performance (typically MHz). Thus, a reduction of the $3D$ simulator in $2D$ is proposed. We assume that the micro-bead will move only in a $2D$ horizontal plane parallel to the electrodes surface at a height equal to its radius R. The impact of this assumption is going to be discussed at the end of the paper. The $2D$ simulator uses a similar approach to the $3D$ DMS presented above. In this $2D$ model, a database of the elementary spacial force is created. This database links the $2D$ dielectrophoretic force directly to the applied voltages, which will reduce sufficiently the computation time. Using the linear relationship between the electric field $\overrightarrow{E}$ and the applied voltages U, the dielectrophoretic force can be written as a second order equation with respect to the electric voltages. Using the electrodes configuration presented in the figure 1, and the following electric voltages vector:

$$U = [U_{ref} - u_x + u_y, 2u_y, U_{ref} + u_x + u_y], \tag{10}$$

the $2D$ dielectrophoretic force $[F_{DEP_x}, F_{DEP_y}]$ can be written as the following:

$$\begin{aligned} F_{DEP_x} &= f_{11}u_x^2 + f_{12}u_y^2 + f_{13}u_x u_y \\ &\quad + f_{14}U_{ref}u_x + f_{15}U_{ref}u_y + f_{16}Uref^2 \\ F_{DEP_y} &= f_{21}u_x^2 + f_{22}u_y^2 + f_{23}u_x u_y \\ &\quad + f_{24}U_{ref}u_x + f_{25}U_{ref}u_y + f_{26}U_{ref}^2. \end{aligned} \tag{11}$$

U_{ref} is a reference voltage, u_x and u_y are the varying voltages and $f_{i,j}$ are spacial functions in x and y essentially dependent on the electrodes geometries. Discrete values of these functions will be computed in a x, y grid points using the $3D$ simulator and stored in a database and a quadratic interpolation is used to evaluate these functions

in an arbitrary (x, y) point. Using this $2D$ numeric model, the $2D$ direct dynamic model becomes:

$$\begin{bmatrix} \dot{x} \\ \dot{y} \end{bmatrix} = \frac{1}{6\pi\nu R} \begin{bmatrix} F_{DEP_x} \\ F_{DEP_y} \end{bmatrix} \quad (12)$$

The weight $\overrightarrow{P}$ has been removed as its projection on the x, y plane is null.

Consequently, the computation time is reduced and few arithmetic iterations are executed in a very short time, even with the interpolation procedure. Indeed, 40 CPU clock cycles are needed to compute the 2 components of the dielectrophoretic force in a grid point, and 180 CPU clock cycle in an interpolated position. In the other hand, using the $3D$ dielectrophoretic force computation, at least 10^4 CPU clock cycle are needed. Thus if we consider that the micro-bead's time response is $3ms$ and for a successful tracking at least 10 control sequence are generated, a controller card with $1MHz$ clock takes $0.2ms$ to compute the dielectrophoretic force using the $2D$ model. The same controller card may takes more then $10ms$ when using the $3D$ dynamic modeling.

III. 2D TRAJECTORY TRACKING

To control the micro-bead's trajectory in a $2D$ dielectrophoretic local periodic structure, an elementary control law for tracking trajectories is presented in this section where a micro-bead moves in one structure. The behavior of a micro-bead in a dielectrophoretic system is characterized by its high dynamics as presented in [16] and the nonlinearity with respect to the applied voltages as shown in the equation (11). This elementary control law must takes into consideration this two problematics. Consequently a simple proportional integrator control is not sufficient especially when the micro-bead approaches the electrodes where the nonlinearity becomes very high. The analytic inversion of the $2D$ model (12) is not possible due to the strong coupling between the control variables u_x and u_y. One way to solve this problem is to use the Newton-Raphson numeric method which is able to find the values of the control variables, u_x and u_y to follow a reference trajectory.

A. 2D Inverse dynamic model

Newton-Raphson is a method for finding successively better approximations to the roots of a real-valued functions. By sampling the $2D$ dynamic model (12) and knowing the trajectory $[\hat{x}(t), \hat{y}(t)]$ with respect to the time we are able to compute the appropriate control variable $u_x(t)$ and $u_y(t)$ using the Newton-Raphson method as illustrated in the figure 5:

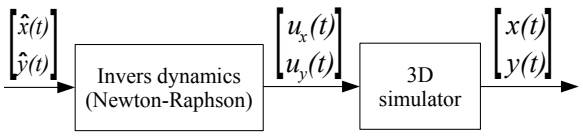

Fig. 5. The Newton-Raphson method is used to find the control variables u_x and u_y

By sampling the dynamic equation (12) using a sampling period T we obtain:

$$\begin{bmatrix} \hat{x}_{k+1} \\ \hat{y}_{k+1} \end{bmatrix} = \frac{T}{6\pi\nu R} \begin{bmatrix} F_{DEP_x}(u_{xk}, u_{y_k}) \\ F_{DEP_y}(u_{xk}, u_{y_k}) \end{bmatrix} + \begin{bmatrix} x_k \\ y_k \end{bmatrix} \quad (13)$$

where $\hat{x}_{k+1}$ and $\hat{y}_{k+1}$ are the next trajectory point at the date kT. Applying the Newton-Raphson method to this model consists in finding iteratively a series of u_x and u_y. At the date kT we have:

$$\begin{bmatrix} u_{x_{k+1}} \\ u_{y_{k+1}} \end{bmatrix} = \begin{bmatrix} u_{x_k} \\ u_{y_k} \end{bmatrix} - J(u_{x_k}, u_{y_k})^{-1} \begin{bmatrix} F(u_{x_k}, u_{y_k}) \\ G(u_{x_k}, u_{y_k}) \end{bmatrix}$$

where u_{x_0} and u_{y_0} are the last computed control variable, J is the jacobin matrix:

$$J(u_{x_k}, u_{y_k}) = \begin{bmatrix} \frac{\partial F(u_x,u_y)}{\partial u_x}\Big|_{u_{x_k},u_{y_k}} & \frac{\partial F(u_x,u_y)}{\partial u_y}\Big|_{u_{x_k},u_{y_k}} \\ \frac{\partial G(u_x,u_y)}{\partial u_x}\Big|_{u_{x_k},u_{y_k}} & \frac{\partial G(u_x,u_y)}{\partial u_y}\Big|_{u_{x_k},u_{y_k}} \end{bmatrix} \quad (14)$$

and

$$\begin{aligned} F(u_x, u_y) &= F_{DEP_x}(u_x, u_y) - 6\pi\nu R(\hat{x}_{k+1} - x_k) \\ G(u_x, u_y) &= F_{DEP_y}(u_x, u_y) - 6\pi\nu R(\hat{y}_{k+1} - y_k) \end{aligned} \quad (15)$$

The iterations clasically stops when:

$$\|u_{x_{l+1}} - u_{x_l}\| \leqslant \delta_u \quad and \quad \|u_{y_{l+1}} - u_{y_l}\| \leqslant \delta_u$$

where δ_u is an error threshold.

B. Numeric application and experimental results

Considering the electrodes geometry presented in the figure 1 submerged in a ultra pure water, where the trajectory of a micro-bead made of silica will be controlled. The table I contains the numeric values of the system physical parameters.

physical parameters	notations	values
vacuum permittivity	ϵ_0	$8,85 \cdot 10^{-12} CV^{-1}m^{-1}$
particle permittivity	ϵ_p	$8,4 \cdot \epsilon_0$
particle conductivity	σ_p	$10^{-12} Sm^{-1}$
medium permittivity	ϵ_m	$80\epsilon_0$
medium conductivity	σ_m	$4.10^{-6} Sm^{-1}$
water volumlic density	$\mathcal{R}_m$	$1000 Kgm^{-3}$
frequency	f	$10KHz$
Clausius-Mossotti	$Re[K(\omega)]$	-0.42

TABLE I
NUMERICAL APPLICATION

Firstly, we are tracking a square reference trajectory with $1s$ period, presented in the figure 6(a).

Applying the Newton-Raphson method, a series of u_x and u_y control variables are computed and presented in the figure 6(b). These computed electric voltages are transmitted to a digital-analogic convertor, then they are amplified and applied to the electrodes where the particle is placed (see figure 7). The micro-bead's position is captured by a high speed camera acquisition at 300 images per seconds.

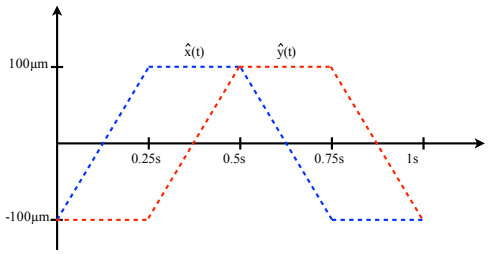

(a) $\hat{x}(t)$ and $\hat{y}(t)$ low speed trajectory.

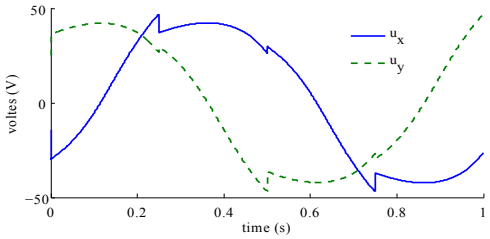

(b) The computed u_x and u_y values for tracking the low speed trajectory.

Fig. 6. The control variable u_x and u_y computed for tracking the low speed trajectory.

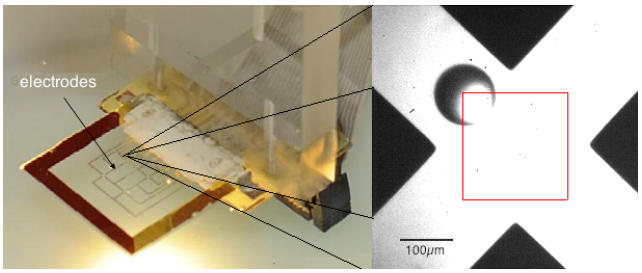

Fig. 7. Experimental electrode used to apply the dielectrophoretic motion. The square presents the reference trajectory.

The figure 8 shows the real trajectory of the micro-bead when applying the u_x and u_y series already computed. The relative error between the real trajectory and the reference is less then 8%. This results shows the ability to control the trajectory of a micro-bead in dielectrophoretic system using open loop control strategy.

IV. Discussion

In order to show the limitation of our current control law a second experiment with a trajectory 10 times faster is studied (figure 9(a)). The $2D$ controller computes a new series of u_x and u_y presented in the figure 9(b). The figure 10 shows the real trajectory of the micro-bead when applying the new u_x and u_y series. As this figure shows, the real trajectory does not follow the reference and the error is bigger then 50%. This is essentially due to the limitation of the $2D$ controller where the dynamic model is limited to $2D$. In reality the micro-bead moves in the three directions x, y and z but in the $2D$ dynamic mode, it supposes to move in a horizontal plane. The main difference between both experiments is the applied voltages u_x and u_y. In the second case, the computed voltage is greater then $50V$.

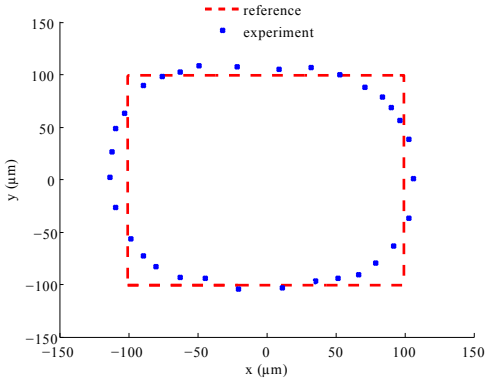

Fig. 8. The real trajectory made by the micro-bead when applying the computed u_x and u_y for the low speed trajectory.

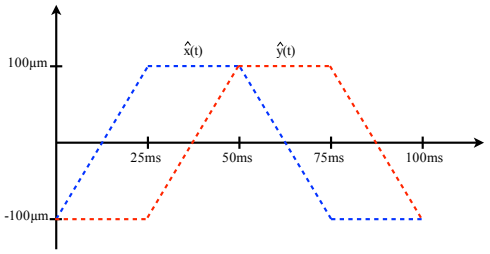

(a) $\hat{x}(t)$ and $\hat{y}(t)$ high speed trajectory.

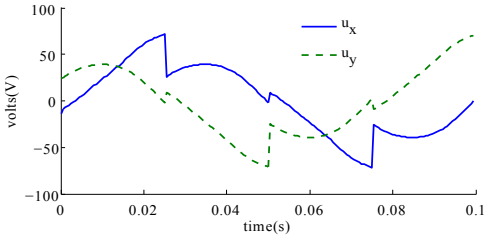

(b) The computed u_x and u_y values for tracking the high speed trajectory.

Fig. 9. The control variable u_x and u_y computed for tracking the high speed trajectory.

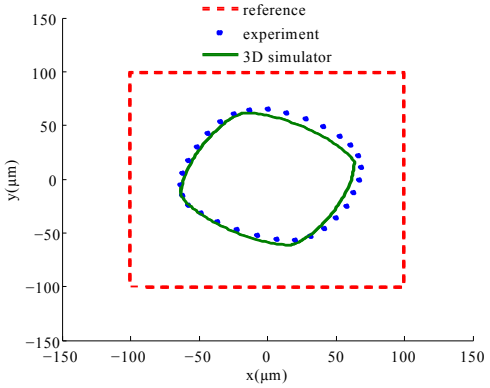

Fig. 10. The real trajectory made by the micro-bead when applying the computed u_x and u_y for the high speed trajectory.

When applying these voltages, experiments show that the height of the micro-beads is significantly different from the

plane assumed in the $2D$ dynamic model. Thus, in the first experiment, the real height of the micro-bead is very close to the plane of the $2D$ dynamic modeling consequently the error between the real trajectory and the reference is less then 8%. In the second experiment, the micro-bead's motion is $100\mu m$ higher than the plane of the $2D$ dynamic model, consequently the error between the real trajectory and the reference is bigger then 50%. However, the object trajectory computed using the $3D$ dynamic model is very close to the experimental measurement (see figure 10). This indicates that our $3D$ simulator is reliable and could be used to develop an new $3D$ control law based on a new simplified $3D$ dynamic model.

The current method proposed in this paper has shown its relevance for low altitude trajectories, the extension of this approach in $3D$ will be developed in future works.

V. Conclusion

In order to control the trajectory of a micro-object for long distance and high speed, an elementary open-loop positioning control for a micro-bead is presented using dielectrophoresis. A $3D$ dielectrophoretic force simulator has been firstly presented. We have shown that the full $3D$ dynamic model is too complex to be introduced in a controller card. Thus a reduced $2D$ dynamic model based on the $3D$ dynamic model was developed. This model is then used to establish a $2D$ control law. We have shown that inverting this model is quite difficult, consequently we have proposed to use the Newton-Raphson numerical method, in order to compute the appropriate control variable with respect to a reference trajectory. Two experiments was presented including two reference trajectories with different speed. Experiments have shown that the $2D$ controller has succeeded to track the low speed trajectory, and failed to track the high speed trajectory. This difference has been also discussed. Experiments also have confirmed that the original $3D$ dynamic modeling is reliable, and could be used in developing a new control law dedicated to $3D$ trajectories.

Acknowledgment

The authors would like to thank all the contributors in this collaborative work under the european project FAB2ASM (contract FoF-NMP-2010-260079): Efficient and Precise 3D Integration of Heterogeneous Microsystems from Fabrication to Assembly, (http://fab2asm.eu/).

References

[1] R. A. Bowling, "A theoretical review of particle adhesion," *Particles on Surfaces*, vol. 1, pp. 129–142, 1988.

[2] Z. R. Gagnon, "Cellular dielectrophoresis: Applications to the characterization, manipulation, separation and patterning of cells," *Special Issue: Dielectrophoresis 2011 – Part II*, vol. 32, no. 18, pp. 2466–2487, 2011.

[3] W. Yan, N. Mechau, H. Hahn, and R. Krupke, "Ultraviolet photodetector arrays assembled by dielectrophoresis of zno nanoparticles," *Nanotechnology*, vol. 21, no. 11, p. 5501, 2010.

[4] K. Onda and F. Arai, "Multi-beam bilateral teleoperation of holographic optical tweezers," *Optics Express*, vol. 20, no. 4, pp. 3633–3641, 2012.

[5] M. Kharboutly, M. Gauthier, and N. Chaillet, "Studing, modeling and controling a dielectrophoresis-based system," PHD thesis, 2011.

[6] M. P. Hughes, *Nanoelectromechanics in Engineering and Biology*. CRC PRESS, 2002.

[7] M. Gel, Y. Kimura, O. Kurosawa, H. Oana, H. Kotera, and M. Washizu, "Dielectrophoretic cell trapping and parallel one-to-one fusion based on field constriction created by a micro-orifice array," *Biomicrofluidics*, vol. 4, p. 022808, 2010.

[8] I.-F. Cheng, V. E. Froude, Y. Zhu, H.-C. Chang, and H.-C. Chang, "A continuous high-throughput bioparticle sorter based on 3d traveling-wave dielectrophoresis," *Lab on a Chip*, vol. 9, pp. 3193 – 3201, 2009.

[9] S. B. A., H. V. R., F. Yolanda, and C. E. B., "Concentration and separation of biological organisms by ultrafiltration and dielectrophoresis," *United States Patent*, vol. 7, p. 439(15), 2010.

[10] H.-H. Cui and K.-M. Lim, "Pillar array microtraps with negative dielectrophoresis," *Langmuir*, vol. 25, pp. 3336–3339, 2009.

[11] S. I. Khondaker, K. Luo, and Z. Yao, "The fabrication of single-electron transistors using dielectrophoretic trapping of individual gold nanoparticles," *Nanotechnology*, vol. 21, p. 095204, 2010.

[12] H. Zhang, J. Tang, P. Zhu, J. Ma, and L.-C. Qin, "High tensile modulus of carbon nanotube nano-fibers produced by dielectrophoresis," *Chemical Physics Letters*, vol. 478, pp. 230–233, 2009.

[13] L. Pan, G. Xiang, L. Huang, Z. Yu, J. Cheng, W. Xing, and Y. Zhou, "Automatic positioning ans sensing microelectrode array (apsmea) for miulti-site electrophysiological recordings," *Journal of Neuroscience Methods*, vol. 170, pp. 123–129, 2008.

[14] N. G. Loucaides, A. Ramos, and G. E. Georghiou, "Micro- and nano-particle manipulation by dielectrophoresis: devices for particle trapping and the influence of steric effects," *physica status solidi*, vol. 5, no. 12, pp. 3794 – 3797, 2008.

[15] R. S. W. Thomas, P. D. Mitchell, R. O. C. Oreffo, and H. Morgan, "Trapping single human osteoblast-like cells from a heterogeneous population using a dielectrophoretic microfluidic device," *Biomicrofluidics*, vol. 4, p. 022806, 2010.

[16] M. Kharboutly, M. Gauthier, and N. Chaillet, "Modeling the trajectory of a micro particle in a dielectrophoresis device." *Journal of Appl. Phys.*, vol. 106, no. 11, pp. 114 312 – 114 312–7, 2009.